Korean Chem. Eng. Res., 56(1), 14-23 (2018)
https://doi.org/10.9713/kcer.2017.56.1.14
PISSN 0304-128X, EISSN 2233-9558

Effect of Dodecylbenzene Sulfonic Acid on the Behavior of Asphaltene Aggregation in a Solvent Deasphalting System

Lingyu Liu*, Kang Seok Go†, Nam Sun Nho, Kwang Ho Kim and Young-Woo Rhee*,‡

Climate Change Research Division, Korea Institute of Energy Research (KIER), 152 Gajeongro, Yuseong-gu, Daejeon, 34129, Korea
**Graduate School of Energy Science and Technology, Chungnam National University (CNU), 99 Daehak-ro, Yuseong-gu, Daejeon, 34134, Korea*
(Received 28 August 2017; Received in revised form 21 September 2017; accepted 22 September 2017)

Abstract – The effect of dodecylbenzene sulfonic acid (DBSA) with different addition amount of DBSA (M_{DBSA}), temperatures and solvent-to-oil ratio (SOR, v/v) on asphaltene aggregation in a solvent deasphalting system was investigated. Increasing the M_{DBSA} at SOR 10 and 55 °C caused the asphaltene removal ratio (ARR) to increase first, then maximize at 1 wt% of M_{DBSA} and then decrease continuously. Based on the SARA (saturate, aromatic, resin, asphaltene) composition, the adsorption amount of DBSA on the asphaltene surface and the self-aggregation of the DBSA, the reason for the change in ARR with M_{DBSA} was found due to the adsorption mechanism. In addition, the asphaltene-resin-DBSA colloidal size confirmed the change of adsorption behavior between the asphaltene and DBSA. Based on the results of this study, a hypothetical adsorption mechanism of DBSA on asphaltene aggregation in the solvent deasphalting system was conceived of and proposed.

Key words: Asphaltene removal ratio, Addition amount of DBSA, The level of self-aggregation of DBSA, Asphaltene colloid size, Adsorption mechanism

1. Introduction

Asphaltene is considered by petroleum engineers to be the most problematic compound to deal with. It is defined to be the fraction of petroleum that is insoluble in normal paraffin solvents, such as n-heptane, and soluble in aromatic solvents like benzene or toluene [1,2]. The flocculation and precipitation of asphaltene cause the plugging of pores of reservoir rocks, bore tubing of wells, pipelines and other auxiliary equipment [3]. Asphaltene is also responsible for the high yield of thermal coke as well as the deactivation of catalysts in catalytic processes [4]. Thus, much research has been conducted to study the chemical structure of asphaltene to understand the mechanisms that cause it to either maintain stability or become unstable, and precipitate in a crude oil system.

Solvent deasphalting (SDA) is a process (mainly developed by KBR and UOP/FW) wherein relatively lighter and more-paraffinic molecular hydrocarbons are physically separated from the heavier poly-condensed aromatic molecules by paraffinic solvent extraction [1]. It is a simple, economical process to remove asphaltene-rich pitch and then send the relatively cleaned-up de-asphalted oil (DAO) to an upgrader process, such as hydrocracking, fluid catalytic cracking (FCC) and so on [5,6]. In general, when the solvent-to-oil ratio (SOR) is decreased, the DAO yield increases with more asphaltene to be produced together [6,7]. This indicates that the SOR has a significant influence on the purification level, meaning that the quality of the DAO can be significantly improved by increasing it. However, doing so requires a copious amount of energy to recover the solvent when a high SOR is used [8]. So, it is necessary to study how to either reduce the amount of solvent or increase the selectively of asphaltene at certain conditions under the premise of guaranteeing a high asphaltene removal ratio (ARR).

It has been known that resin plays an important role in the stability of asphaltene by attaching its polar head to the asphaltene polar sites and stretching the aliphatic group outward. As a result, the non-polar layer of the resin surrounds the asphaltene surface to prevent its aggregation [2-4,9-11]. For this reason, model resins, especially alkylbenzene-derived surfactants whose structure is similar to natural resins, are studied to find the optimal inhibitor and mechanism of interaction between asphaltene and surfactants [9,11]. Previous studies have stated that the adsorption behavior and chemical structure of surfactants play an important role in stabilizing asphaltene [2-3,12-14]. It has also been proposed that, among the numerous inhibitors available, dodecylbenzene sulfonic acid (DBSA) is a prominent stabilizer due to its high polarity of the head group, long alkyl chain and large adsorption amount on the asphaltene surface [13-16].

On the other hand, the enhancement of asphaltene aggregation by an addition of DBSA has been reported by Goual and Firoozabadi. They found that DBSA can help to increase asphaltene aggregation, but only up to certain point. Over a certain concentration, the aggregation was found to decrease [17]. However, neither the reason nor the mechanism for this retrograde phenomenon was identified.

† To whom correspondence should be addressed.
E-mail: ksgo78@kier.re.kr, ywrhee@cnu.ac.kr

Fortunately, the interaction between DBSA and asphaltene and the DBSA adsorption mechanism on asphaltene surface have been studied copiously. Chang and Fogler employed Fourier transform infrared (FT-IR) to investigate the interaction between asphaltenes, p-alkylphenol and DBSA with the results indicating that asphaltene has a complicated acid-based interaction with DBSA with a stoichiometry of about 1.8 mmol of DBSA/g of asphaltene [15]. Leòn et al. determined the adsorption process of DBSA on the asphaltene surface by isotherm, and due to the plateaus of the two curves of adsorption isotherm, the two steps of the adsorption process were found as follows: In the first step, DBSA adsorbs on the asphaltene surface by acid-base interactions; in the second step, the interactions between adsorbed DBSA become predominant and the formation of aggregates on the surface begins [12]. Rogel and Leòn improved the adsorption process of DBSA on asphaltene surface by using molecular dynamics, with their results revealing how the two steps corresponding to low and high coverage of DBSA on asphaltene occur. They explained that at low coverage, DBSA prefers a perpendicular configuration to the asphaltene surface due to the acid-base interaction, while at high coverage the DBSA heads will lie parallel to the asphaltene surface with their tails extending isotropically toward the heptane [3]. Recently, Wei et al. applied isothermal titration calorimetry (ITC) to study the interaction mechanism between asphaltene and inhibitors (DBSA and nonylphenol). Based on the discovery of the maximum and minimum net heat per mol of DBSA in xylene, they found the concentrations of self-aggregation transition of DBSA. Finally, they proposed that the interaction between DBSA and asphaltene is dependent on the self-aggregation of DBSA as well as the concentration of asphaltene [18].

Our main objective was to find the effect of DBSA on the improvement of asphaltene removal and propose a mechanism of asphaltene aggregation with the DBSA. To do these, the effect of extraction temperature, SOR, and additional amount of DBSA (M_{DBSA}) on the selective removal of asphaltene was investigated first. A hypothetical mechanism of asphaltene behavior with DBSA was proposed based on an analysis of adsorption behavior, the level of self-aggregation of DBSA, and the change of asphaltene-resin-DBSA colloid size as a function of M_{DBSA}.

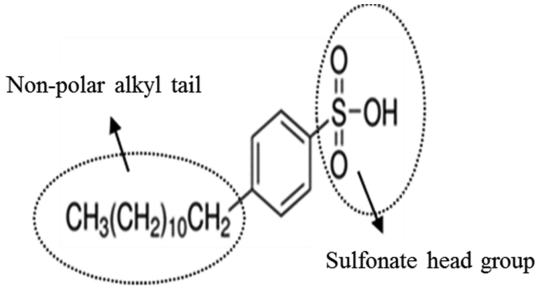

Fig. 1. Chemical structure of DBSA.

2. The Experiment

2-1. Materials

Canadian Athabasca oil sand bitumen (properties see Table 1) was used for feedstock. DBSA (90%, Sigma-Aldrich) and n-Heptane (98%, Sigma-Aldrich) were used to form the DBSA solution with varying addition amounts of DBSA (M_{DBSA}, based on the weight of the feed). The chemical structure of the DBSA is as shown in Fig. 1.

2-2. Experiment procedure

First, a series of DBSA solutions was prepared by n-heptane and DBSA. As given SOR, each DBSA solution was mixed with the bitumen in Erlenmeyer flask. The mixture was stirred by magnetic stirrer and let settle for 30 minutes and one hour at the desired temperature, respectively. After filtration using 0.45 μm filter paper, the filtered materials were dried at 107 °C for over 4 hours, and then the remaining materials were taken as pitch. The pitch yield was obtained from the weight percentage of pitch divided by feed weight. Details of the experiment are presented in Fig. 2(a) and Table 2. The asphaltene content in pitch was obtained from the weight percentage of n-heptane insoluble asphaltene (SOR 100) divided by pitch weight as ASTM D3279 [19]. The procedure is shown in Fig. 2(b).

The asphaltene removal ratio (ARR) used as an indicator for the selective removal of asphaltene was calculated by Eq. (1):

$$\text{Asphaltene removal ratio, ARR (wt\%)} = \frac{\text{Pitch yield} \times \text{Aspaltene content in pitch}}{\text{Asphaltene content in feed}} \quad (1)$$

Table 1. Properties of bitumen

Properties	Values	Remarks
Elemental analysis, wt%	C: 83, H: 10.3, N: 0.5, S: 5.2, O: 0.9	
Mass of fractions, wt% /Cut point, °C	Naphtha: 0/0-177 °C Middle distillate: 13.5/177-343 °C Vacuum gas oil: 39.03/343-524 °C Vacuum residue: 47.47/>524 °C	ASTM D 7169
MCR content, wt%	14.48	ASTM D 4530
Heavy metal content, ppm	Ni: 105, V: 195	ASTM D 4294
Viscosity/mPa.s	240-46,400	Temperature Range: [35-100 °C]
API gravity	8.18	ASTM D 287
SARA analysis, area%	Saturate/Aromatic/Resin/Asphaltene: 8.8/52.8/21.4/17.6	IP 469-01

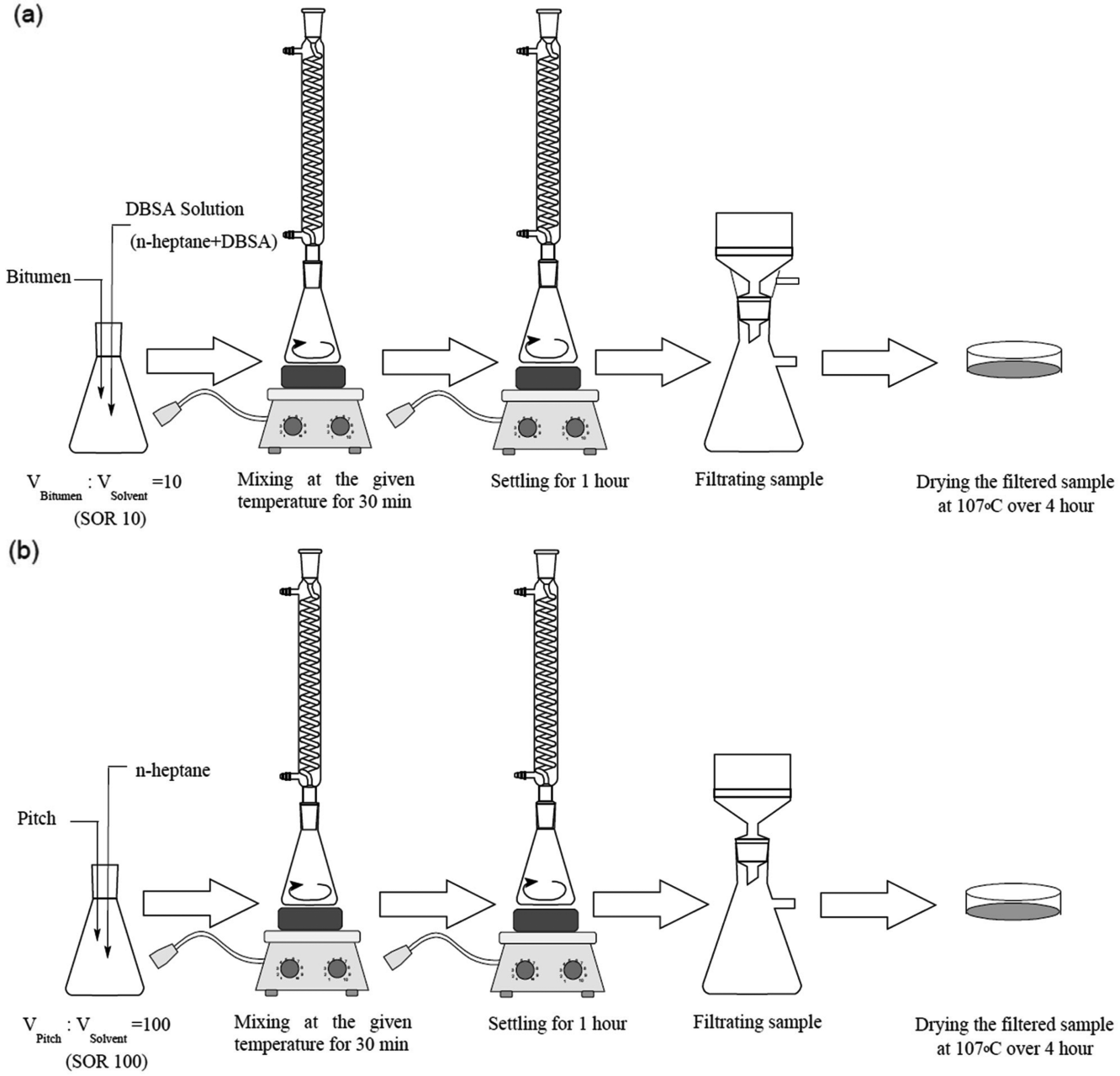

Fig. 2. Experimental procedures (a) for solvent deasphalting, (b) for the measurement of asphaltene content in the samples.

Table 2. Experimental conditions

Bitumen (g)	M_{DBSA} (wt%)	Solvent to oil ratio (SOR) (v/v)	Temperature (°C)
4.9	1	3	55, 75, 90
4.9	1	5	55, 75, 90
4.9	0.5	10	55
4.9	1	10	55, 75, 90
4.9	2	10	55
4.9	3	10	55
4.9	5	10	55
4.9	7	10	55

Each condition was carried out in at least six parallel tests with the data, except the highest and lowest, used to calculate the average ARR value that was then applied to study the effect of DBSA on asphaltene aggregation. In this study, we designated the samples without any addition of DBSA as a 'reference case'.

2-3. Analysis

2-3-1. SARA analysis

SARA (saturate, aromatic, resin, asphaltene) analysis divides petroleum components based on their polarizability and polarity [20,21]. Based on the IP 469-01 standard, the distribution of resin content in pitch was measured by the TLC/FID Analyzer (IATROSCAN MK-6s) in this study.

2-3-2. X-ray photoelectron spectroscopy (XPS) analysis

The relative adsorbed amount of DBSA on the asphaltene surface

Table 3. Binding energy of sulfur group types in asphaltene

Croup types	Binding energy/eV	Reference
Sulfonate	167.7	[22]
Sulphoxide	165.8	[23]
Thiophenic	164.2-164.5	[24-26]
Aliphatic	163.3-163.4	[24, 25]

was determined by XPS. The binding energy of carbon 1s at 284.8 eV was used to eliminate the charging effect. The types of sulfur group and binding energy are presented in Table 3.

2-3-3. UV-Vis spectroscopy

Shimadzu UV-Vis spectrophotometer was employed to find the critical inverse micellization concentration of the DBSA ($CIMC_{DBSA}$) in heptane [16]. The λ_{max} of the DBSA was found to be 261 nm. The average adsorption (Abs) of each DBSA solution at concentration ranges from 0 to over 3,600 ppm was determined by UV-vis at 20 °C and 55 °C, respectively.

2-3-4. Dynamic light scattering

A Malvern Nanosizer ZS was employed to evaluate the variation of the sizes of the asphaltene colloids [27,28]. First, 0.025% w/v of each sample was dissolved in a heptane/toluene mixture at a heptane concentration of 40% w/v (in this part of the experiment, the sample needed to first be dissolved in the toluene with the heptane added immediately afterward). After sitting for about 48 hours, the test sample was taken from the supernatant to be measured for size.

3. Results and Discussion

3-1. Effects of M_{DBSA}, temperature, and SOR on ARR

Fig. 3 shows the effect of M_{DBSA} on the ARR at SOR 10 and at 55 °C. ARR first increases as M_{DBSA} increases up to 92 wt% at 1 wt% of M_{DBSA}. This indicates that a more selective removal of asphaltene can be achieved simply by adding DBSA. However, over 1 wt% of M_{DBSA}, ARR then continuously decreases. When compared to the reference case (0 wt% of M_{DBSA}), at over 3 wt% of M_{DBSA}, ARR can be seen to be lower. It means that DBSA shows dispersion effect on asphaltene aggregation. In this phase, there must be a certain M_{DBSA} that causes the ARR to be the same with the reference case; for this study, it was designated as α wt%. This means that the characteristic of asphaltene aggregation changes in relation to M_{DBSA}, and that the dispersion of asphaltene can be rather enhanced over a certain M_{DBSA}.

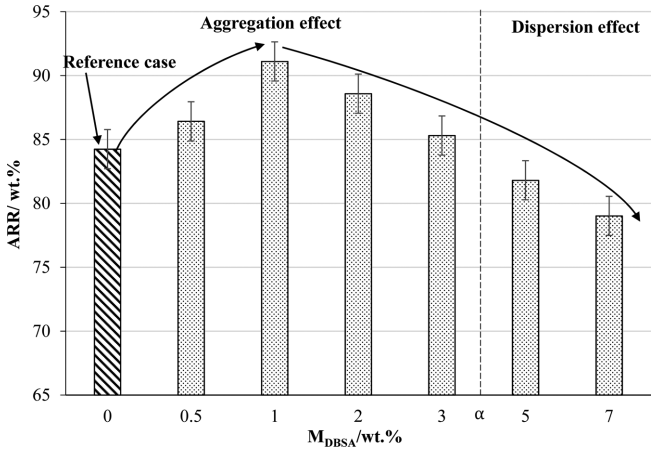

Fig. 3. Effect of M_{DBSA} on ARR at SOR 10 and 55 °C.

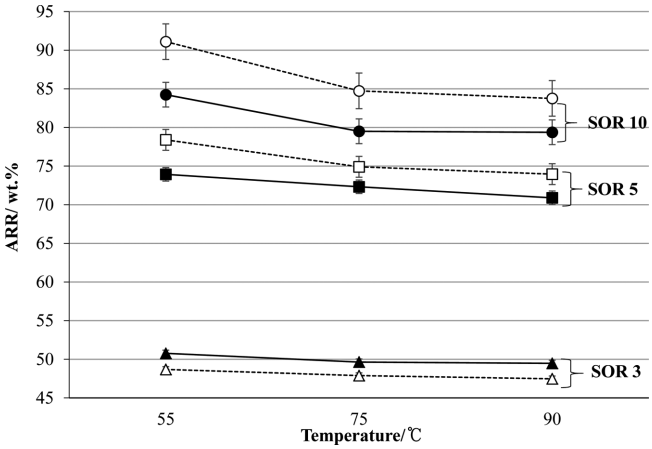

Fig. 4. Effect of temperature and SOR on ARR (solid sample: reference case; empty sample: with 1 wt% of M_{DBSA}).

The effect of extraction temperature and SOR on ARR at the point of highest effect of M_{DBSA} (1 wt%) is shown in Fig. 4. ARR decreases with the increase of temperature and decrease of SOR. Also, the ARR at SORs 5 and 10 was higher than the reference throughout the temperature range. This means that at SORs 5 and 10 that asphaltene aggregation is enhanced by the addition of DBSA. However, a distinct phenomenon is observed at SOR 3. Unlike at either SOR 5 or 10, the asphaltene removal ratio at SOR 3 is rather lower than the reference case.

Based on the results that can be seen in Fig. 3 and Fig. 4, it can be suspected that the behavior of asphaltene aggregation might be related to the DBSA adsorption on the surfaces of the asphaltene which have different SARA compositions according to the change of SOR. To find the cause, the changes of resin content and relative adsorption amount of DBSA on asphaltene in pitch with respect to SOR at 55 °C were examined using both SARA and XPS analysis, as shown in Fig. 5.

In Fig. 5, the resin content in pitch increases with the decrease of SOR at the same temperature. The resin content at SOR 3 is shown to be higher than that at both SOR 5 and 10. The relative adsorption amount of DBSA on the asphaltene surface also increases with the decrease of SOR, and a significantly higher relative adsorption amount of DBSA at SOR 3 than at SORs 5 and 10 is clearly observed. Considering the facts depicted in Fig. 4, it can be known that DBSA will cooperatively interact with resin to promote asphaltene dispersion when the resin content in the pitch and adsorbed DBSA on the asphaltene surface is high enough. From literature [4,29-31], the peptization mecha-

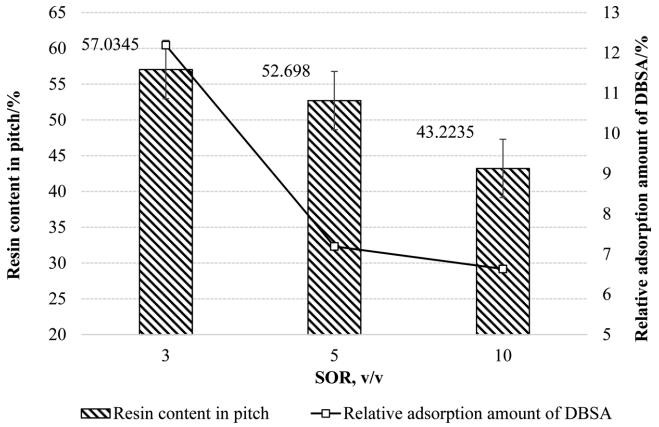

Fig. 5. Resin content in pitch (reference case) and relative adsorption amount of DBSA on asphaltene surface (M_{DBSA}=1 wt%) as function of SOR at 55 °C.

nism of resin is known to help stabilize asphaltene in crude oils by preventing the asphaltene from agglomerating in a steric manner. Also, the DBSA monomers prefer to self-aggregate as the DBSA concentration increases, and the DBSA polymer adsorbed on the asphaltene surface will cause a high amount of DBSA adsorption and form a non-polar multilayer which prevents asphaltene aggregation [9,18]. Thus, at the same additional amount of DBSA, a lower SOR not only causes a higher content of resin in the pitch, but also causes a high level of self-aggregation of DBSA, both of which will form a thick non-polar layer on the asphaltene surface so that asphaltene aggregation is prevented.

3-2. Mechanism of DBSA on asphaltene aggregation

Chang and Fogler suggested that DBSA stabilizes asphaltene by forming multilayers on the asphaltene surface according to significant changes of the asphaltene SAXS curve, which relates to the changes of asphaltene colloid size, in the presence of DBSA [15]. Rogel and Leòn also came to the same conclusion in their study of the adsorption of DBSA on asphaltene surfaces using molecular dynamic simulations, in which they found a significant larger size of DBSA-asphaltene colloid present [3]. So, based on the changes of ARR in Fig. 3, the adsorption amount of DBSA on the asphaltene surface, the level of self-aggregation of DBSA and the changes of asphaltene-resin-DBSA colloidal size were investigated to explain the mechanism of M_{DBSA} on asphaltene aggregation, as follows.

3-2-1. Adsorption behavior of DBSA on the asphaltene surface

As shown in Fig. 6, XPS analysis of sulfur 2p peaks provides detailed information on the sulfur types present on the asphaltene surface [32]. In Fig. 6(a), sulfoxide, thiophenic S and aliphatic S, are divided in the sulfur 2p fitted peak curves of the reference case. However, when DBSA was added a sulfonate group occurred, as shown in Fig. 6(b). Based on the sulfonate peak area, the changes of relative adsorption amount of DBSA on the asphaltene surface as a function of M_{DBSA} at SORs 10 and 55 °C are shown in Fig. 7. The result

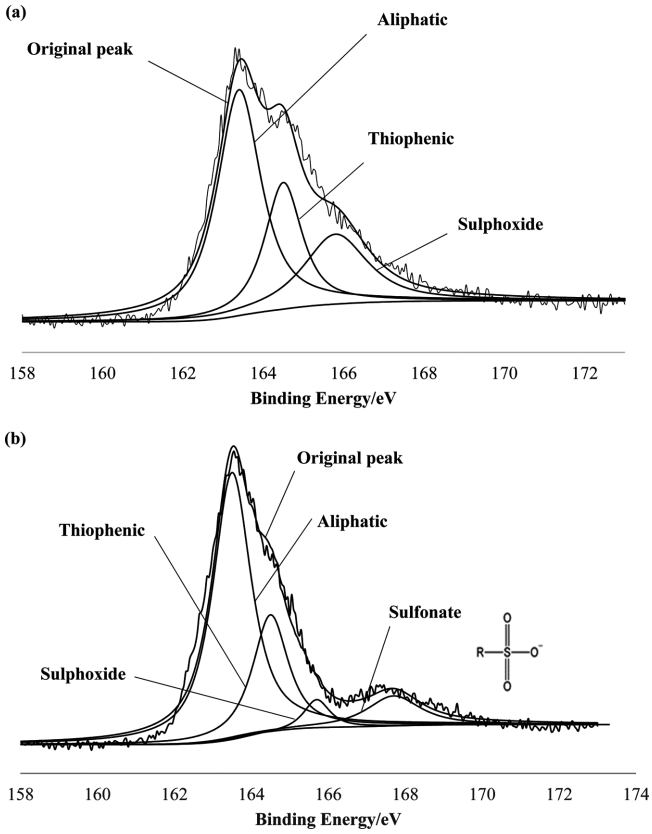

Fig. 6. XPS S2p fitting peak curves of asphaltene at SOR10, 55 °C; (a) reference case; (b) with 1 wt% of M_{DBSA}.

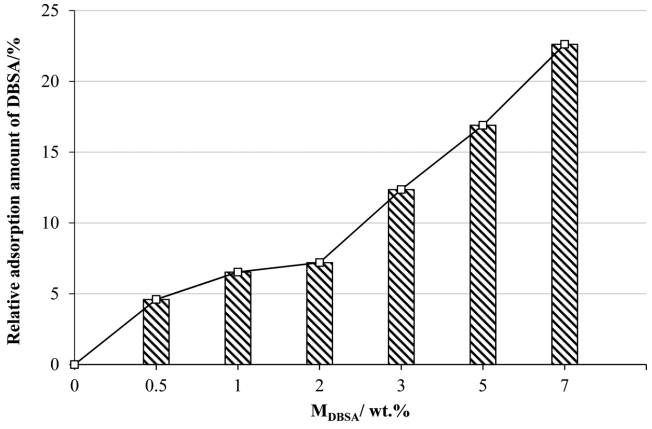

Fig. 7. Relative adsorption amount of DBSA on asphaltene surface with varying M_{DBSA}, SOR 10 and 55 °C.

shows that the adsorbed DBSA on the asphaltene surface increases with the increase of M_{DBSA}, especially above M_{DBSA}=2 wt%, the slope sharply increases. Combining the change of adsorption amount of DBSA with ARR, we speculated that DBSA might form a low coverage on the asphaltene surface during 0 wt% to 1 wt% and after that it changed to be high coverage.

DBSA is a strong organic acid that can protonate heteroatomic nitrogen, oxygen and sulfoxide groups in asphaltene, and sulfonate can protonate N-H to form an acid-based interaction with asphaltene as well [33]. According to Chang and Fogler, asphaltene has a com-

plicated acid-based interaction with DBSA with a stoichiometry of about 1.8 mmol of DBSA/g of asphaltene [13,15]. Rogel and Leòn also observed that even at high DBSA concentrations, the atoms of the head groups are restricted to a narrower region near the asphaltene surface [3]. Based on the value of relative adsorption amount of DBSA (in Fig. 7) and the increase of ARR from 0 wt% to 1 wt% of M_{DBSA}, we can infer that the adsorbed polar DBSA, by acid-base interaction, might increase the polarity of asphaltene and cause the attraction between asphaltene molecules to increase. However, there is a limited site on the asphaltene surface for supporting acid-base interaction with DBSA, so ARR increases first until the site is nearly fully filled (low coverage) at near M_{DBSA}=1 wt% where the highest ARR is present. Then, as the M_{DBSA} continuously increases, the high coverage of DBSA is attributed to formation of a non-polar multilayer which prevents asphaltene aggregation. However, it follows a different mechanism from the one at low coverage. To explain this, the level of self-aggregation of DBSA is considered in the next section.

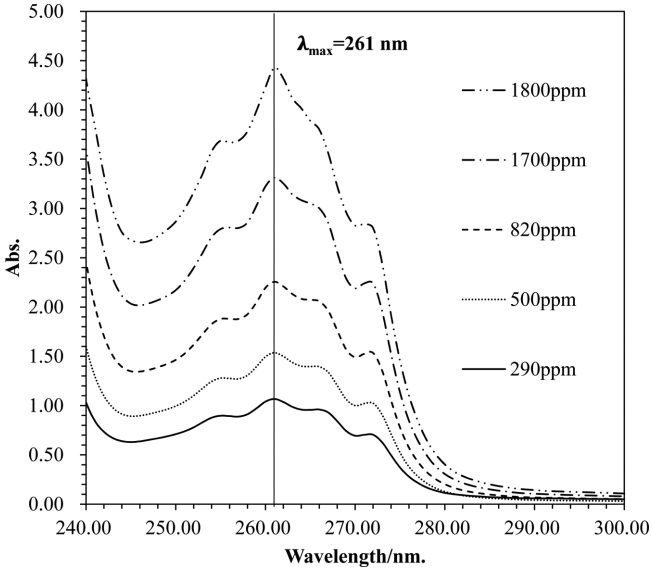

Fig. 9. UV-Vis spectrums with varying DBSA concentration in heptane.

3-2-2. Level of self-aggregation of DBSA in heptane

Critical micellization concentration (CMC) is defined as the concentration of surfactants above which micelles will form [34,35], so it is one of the methods used to classify the level of self-aggregation of surfactants. Zhang et al. found two CMC_{SDBS} with an increase of SDBS concentration by employing UV-Vis spectroscopy and synchronous fluorescence spectroscopy to determine the CMC of sodium dodecyl benzene sulfonate (SDBS) [36]. Different from micelles, an inverse micellization will be formed in a non-polar media [34]. After a certain concentration is exceeded (in this study referred to as critical inverse micellization concentration (CIMC)), DBSA will form in inverse micelles in a non-polar system. As shown in Fig. 8, CIMC can be used to classify the level of self-aggregation of DBSA in n-heptane. DBSA, which exists mostly in the form of a monomer below $CIMC_1$, will aggregate to be either a dimer or multimer between $CIMC_1$ and $CIMC_2$, and, lastly, over $CIMC_2$ it starts to form inverse micelles.

In this study, UV-Vis was employed to find the level of self-aggregation of DBSA in heptane. As shown in Fig. 9, DBSA has a strong signature in the region ranging from 240 nm to 280 nm, and a λ_{max}=261 nm, which is used to set the absorption wavelength of the UV-Vis instrument before measuring the average absorption (Abs) of each DBSA solution. However, temperature has an influence on the level of self-aggregation of DBSA, so the curves of the Abs of each DBSA solution at 20 °C and 55 °C are found in Figs. 10 and 11, respectively. In Fig. 10, three slopes and two points of intersection can be observed with the increase of concentration of DBSA solution at 20 °C. This means that the occurrence of two $CIMC_{DBSA}$, which relates to the transition of self-aggregation of DBSA, results from an increase of concentration of DBSA solution as in previous literature [18]. Based on this figure, we can expect that below $CIMC_1$, DBSA monomers are dominant first; as the concentration increases from $CIMC_1$ to $CIMC_2$, DBSA monomers, dimers and multimers coexist together with the multimers being the main components as the concentration increases; above $CIMC_2$, an inverse DBSA micelle starts to form and the number continuously increases as the concentration increases.

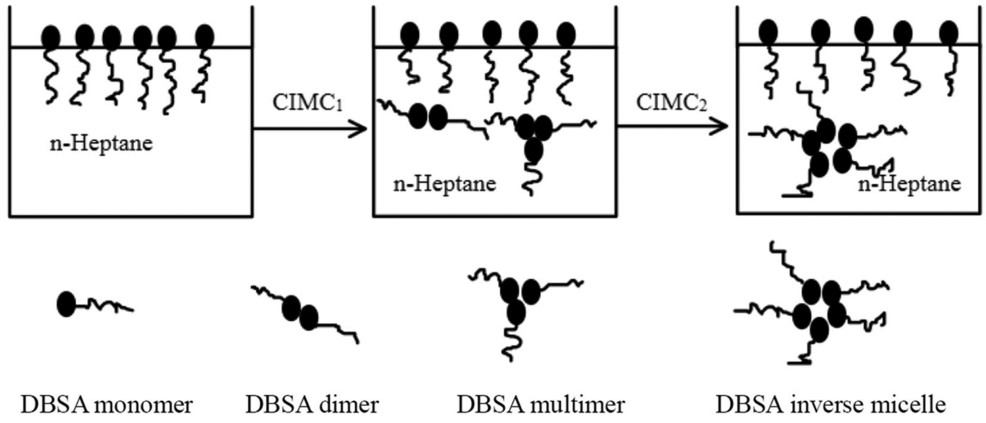

Fig. 8. Level of self-aggregation of DBSA in heptane.

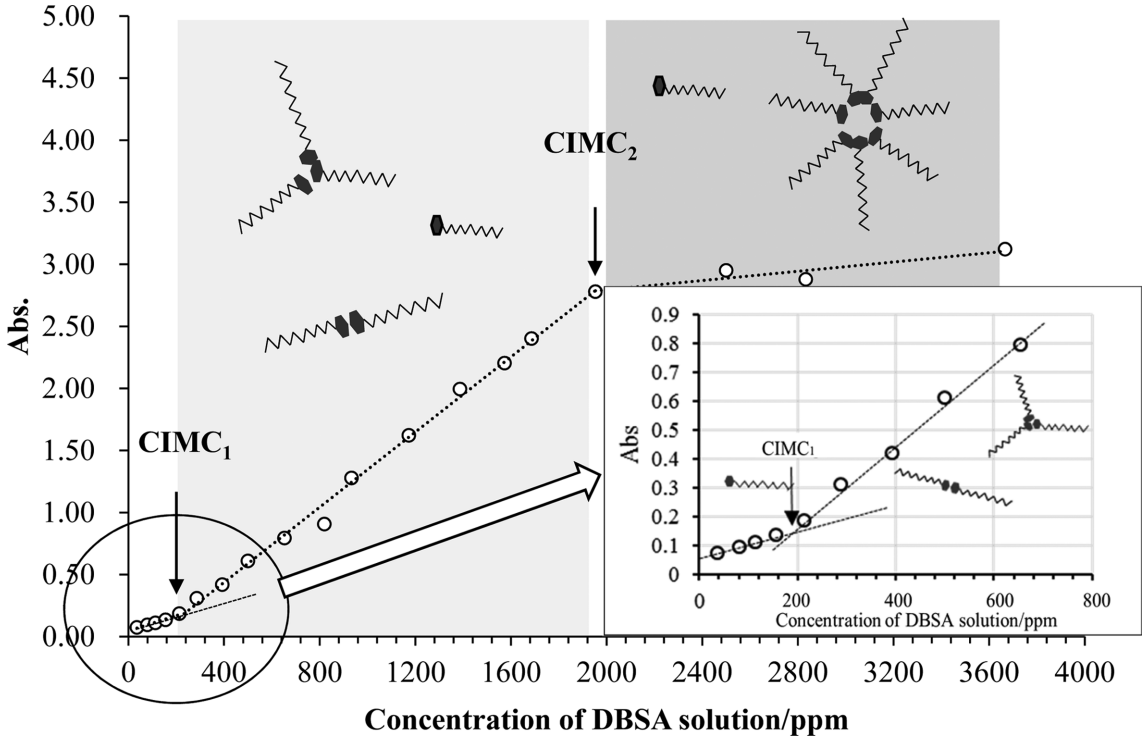

Fig. 10. Change of average Abs of DBSA solution at λ_{max}=261 nm and 20 °C.

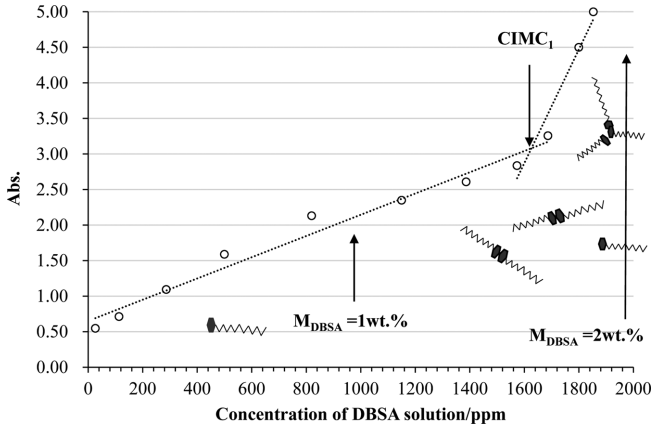

Fig. 11. Change of average Abs of DBSA solution at λ_{max}=261 nm and 55 °C.

The influence of temperature on this self-aggregation behavior is shown in Fig. 11. As can be seen, the $CIMC_1$ near 200 ppm in Fig. 10 is delayed to near 1,630 ppm. However, UV-Vis could not measure much more than 1,800 ppm due to the limitation of the Abs range being lower than 5, so that $CIMC_2$ at 55 °C could not be found using UV-Vis. However, it can be known that below 1 wt% of M_{DBSA} that DBSA will exist mainly in the form of monomers, and at over 2 wt% it starts to form dimers or multimers.

Considering previous studies [3,12,15], there are two steps of adsorption procedure with the multilayer DBSA formed on the asphaltene surface with the high coverage. In this respect, we can propose that DBSA monomers adsorb on the asphaltene surface to form a low DBSA coverage at 0-1 wt% of M_{DBSA}; DBSA prefers to form inverse micelles at over 2 wt% of M_{DBSA} because the interior polar groups of DBSA associate with asphaltene by acid-base interaction with the exterior non-polar tail extended toward heptane. The DBSA inverse micelles adsorb on the asphaltene surface by hydrophobic interaction [37] to form a high DBSA coverage (multilayer) which enhances the solubility of the asphaltene in a solvent deasphalting system; and during the period of DBSA change from monomer to inverse micelle, the non-polarity of the multimer increases as the M_{DBSA} increases.

3-2-3. Change of asphaltene-resin-DBSA colloid size according to adsorption of DBSA

To confirm the change of adsorption behavior between asphaltene

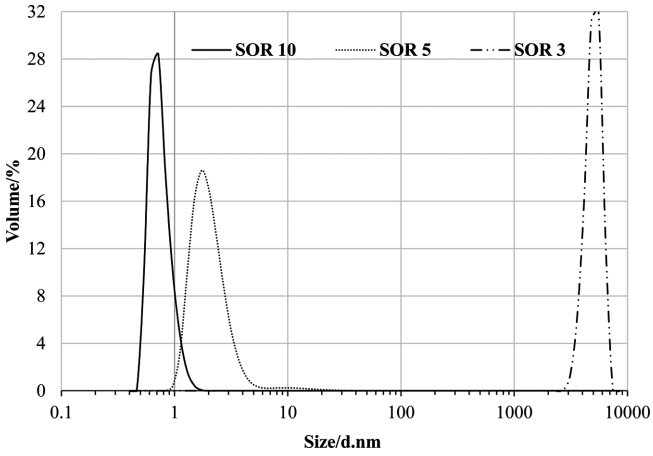

Fig. 12. Asphaltene-resin colloid size with SOR of 3, 5, 10 without DBSA.

and DBSA, the variation of the asphaltene-resin colloid size at SORs 3, 5 and 10 was investigated first as shown in Fig. 12, and the asphaltene-resin-DBSA colloid size as a function of M_{DBSA} is shown in Fig. 13. In Fig. 12, the difference of the asphaltene-resin colloid size distribution at SORs 3, 5 and 10 without addition of DBSA is first observed as increasing with the decrease of SOR with a significantly larger size presenting at SOR3. Considering Figs. 4 and 5 where a lower SOR leads to a higher resin content in the pitch and lower ARR, this means that the higher resin content in the pitch causes a thicker resin layer to cover the asphaltene surface. This layer not only increased the asphaltene-resin colloid size, but also improved the asphaltene stability in a non-polar system.

Fig. 13(a) presents the distribution of the sizes of the asphaltene-resin-DBSA colloids as a function of M_{DBSA}. It shows that the size of the asphaltene-resin-DBSA colloid decreases from 0.5 wt% to 1 wt% of M_{DBSA}, and then increases with the further increase of M_{DBSA}. Especially at the concentrations of 5 wt% and 7 wt%, the size of the colloid sharply increases compared with other concentrations. In particular, different colloid size distribution peaks coexist in the same system (2 wt% and 3 wt% of M_{DBSA}). The explanation can be that the state of DBSA was transitional from dimers to multimers based on the data that can be seen in Fig. 11. This is consistent with Fig. 8 which shows that during the transition from $CIMC_1$ to $CIMC_2$ different levels of DBSA polymer coexist together. Similar to the behavior of DBSA in heptane (Fig. 11), DBSA exists in the form of monomers from 0 wt% to 1 wt% of M_{DBSA} in the solvent deasphalting system, and also the different levels of self-aggregation of DBSA will coexist at over 2 wt% of M_{DBSA}. At over $CIMC_2$, an inverse micelle will occupy the main components in the non-poly system. We additionally know that the formation of a thicker non-polar multilayer is caused by the increasing high level of self-aggregation of DBSA adsorbed on asphaltene surface.

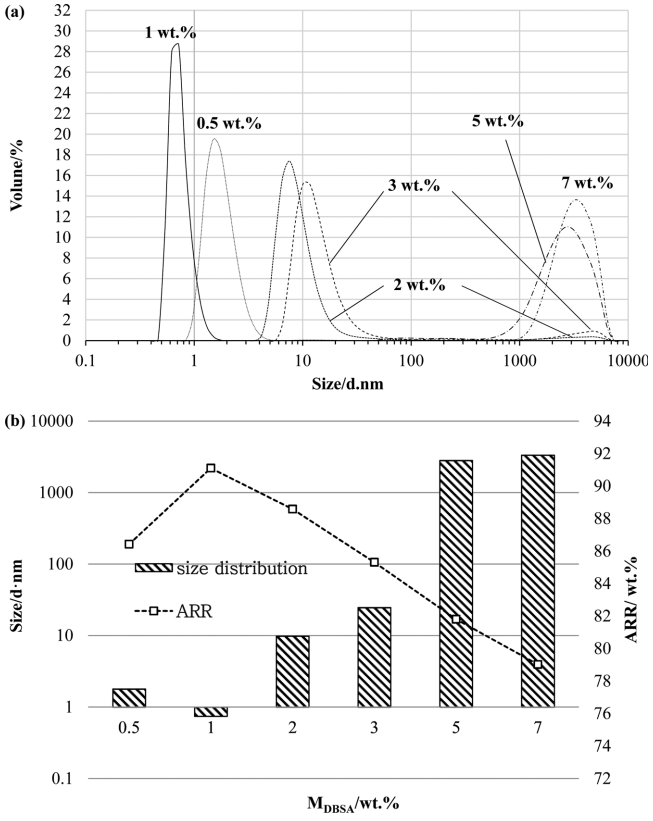

Fig. 13. Asphaltene-resin-DBSA colloid main size distribution at SOR 10, 55 °C. (a) with varying M_{DBSA}; (b) the relation between ARR and colloid size.

Fig. 13(b) shows the correlation between ARR and the main distribution size. The data show that that the size of asphaltene-resin-DBSA colloid is inversely proportional to its removal ratio. Significantly, the lowest size distribution was found to be at the same point as the highest ARR (1 wt% of M_{DBSA}). Combining this result with the self-aggregation of DBSA, the adsorbed DBSA monomer, by acid-base interaction with asphaltene, increases the attraction between asphaltene molecules. This attraction causes the asphaltene-resin-DBSA colloid to form much more tightly. However, the basic site for the formation of the acid-base interaction on the asphaltene surface is fully filled at near 1 wt% of M_{DBSA}.

3-2-4. Hypothetical mechanism of DBSA on asphaltene aggregation as a function of M_{DBSA}

Considering the level of self-aggregation of DBSA, the asphaltene-resin-DBSA colloid size and the changes of ARR at different M_{DBSA}, a hypothesis can be proposed to interpret the effect of the DBSA on asphaltene aggregation, as shown in Fig. 14. In the first step (refer to (a)), DBSA monomers adsorb on asphaltene surface by acid-base interaction until the limited site is filled at 1 wt% of M_{DBSA}. This might cause the attraction between asphaltene molecules to be enhanced which leads asphaltene molecules to cluster tightly, so that the lowest size distribution presents the same point with the highest ARR (1 wt% of M_{DBSA}). In the second step (refer to (b)) above 1 wt% of M_{DBSA}, DBSA dimmers and multimers will, respectively, occupy the main position as M_{DBSA} increases. After DBSA monomers interact with the asphaltene, the excess of non-polar DBSA dimers and multimers, which serves as a resin, will be adsorbed on the asphaltene surface due to hydrophobic interaction and weaken the attraction between asphaltenes. As the M_{DBSA} continuously increases, a non-polar multilayer of DBSA on the asphaltene surface will be completed (refer to (c)). It increases the asphaltene-resin-DBSA size and prevents the aggregation between the asphaltene molecules in the solvent deasphalting system.

4. Conclusion

The effect of DBSA on the behavior of asphaltene aggregation in a solvent deasphalting system was investigated. It was found that 1 wt% of M_{DBSA} is the optimum condition for improving asphaltene aggregation at SOR of 10. Also, at the same M_{DBSA}, either a decrease of temperature or increase of SOR promoted asphaltene aggregation. However, unlike an SOR of 5 or 10, asphaltene dispersion occurred

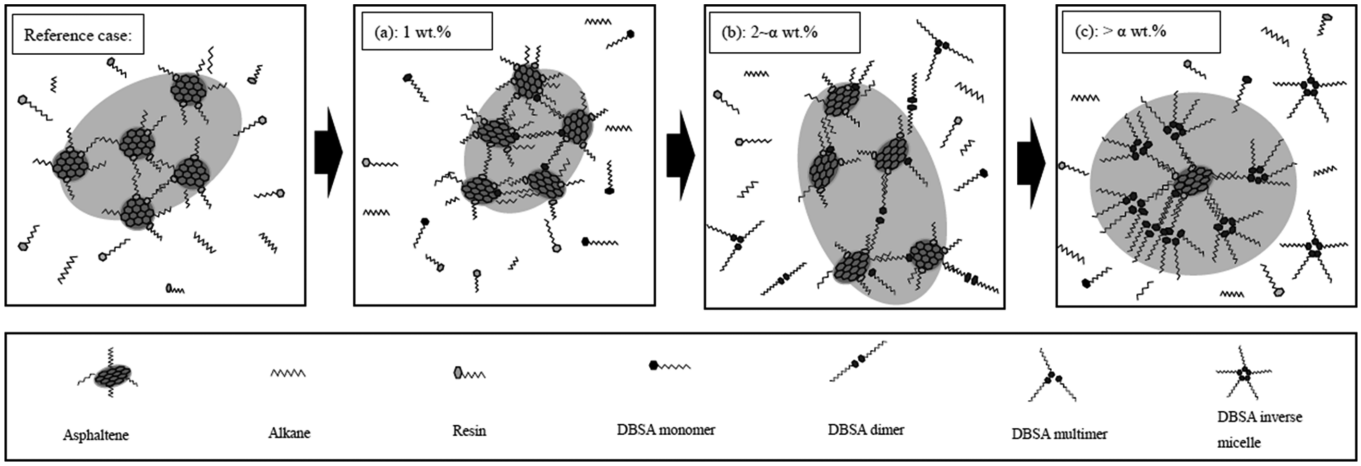

Fig. 14. Schematic diagram of a hypothetical mechanism of DBSA promoting and hindering asphaltene aggregation in the solvent deasphalting system.

at SOR 3 in which the resin is relatively rich.

The behavior of asphaltene aggregation with DBSA was found in terms of the DBSA adsorption amount, DBSA self-aggregation, and asphaltene-resin-DBSA colloidal size. The adsorbed DBSA monomer on asphaltene surface enhances the attraction between asphaltene molecules, which improves ARR. As M_{DBSA} increases, DBSA dimers and multimers serve as a sort of resin for improving asphaltene solubility. At high M_{DBSA}, the adsorbed DBSA inverse micelle forms a non-polar multilayer on asphaltene surface. It results in the increase of asphaltene-resin-DBSA colloid size and enhancement of asphaltene solubility. Based on these findings, a hypothetical mechanism of DBSA that effects asphaltene aggregation was proposed.

Acknowledgments

We would like to acknowledge the financial support from the R&D Convergence Program of NST (National Research Council of Science & Technology) of the Republic of Korea (Grant B551179-12-07-00).

References

1. Banerjee, D. K., Oil Sands, Heavy oil & Bitumen from Recovery to Refinery, Penn Well Corp., USA, 3-10, 101-112(2012).
2. Al-Sahhaf, T. A., Fahim, M. A. and Elkilani, A. S., Retardation of asphaltene precipitation by adding of toluene, resins, deasphalted oil and surfactants, *Fluid Phase Equilib.*, **194-197**, 1045-1057(2002).
3. Rogel, E. and LeÓn, O., "Study of the Adsorption of Alkyl Benzene-derived Amphiphiles on an Asphaltene Surface Using Molecular Dynamic Simulation," *Energy Fuels*, **15**(5), 1077-1086(2001).
4. Andersen, S. I. and Speight, J. G., "Petroleum Resins: Separation, Character, and Role in Petroleum," *Pet. Sci. Technol.*, **19**(1-2), 1-34(2001).
5. Lee, J. M., Shin, S., Ahn, S., Chun, J. H., Lee, K. B., Mun, S., Jeon, S. G., Na, J. G. and Nho, N. S., "Separation of Solvent and Deasphalted Oil for Solvent Deasphalting Process," *Fuel Process. Technol.*, **119**, 204-210(2014).
6. Huc, A. Y., Heavy Crude Oils: from Geology to Upgrading an Overview, Editions Technip, France, 231-256(2011).
7. Alboudwarej, H., Beck, J., Svrcek, W. Y. and Yarranton, H. W., "Sensitivity of Asphaltene Properties to Separation Techniques," *Energy Fuels*, **16**(2), 462-469(2002).
8. Ahn, S., Shin, S. S., Im, S. I., Lee, K. B. and Nho, N. S., "Solvent Recovery in Solvent Deasphalting Process for Economical Vacuum Residue Upgrading," *Korean J. Chem. Eng.*, **33**(1), 265-270(2016).
9. Pan, H. and Firoozabadi, A., "Thermodynamic Micellization Model for Asphaltene Precipitation Inhibition," *AIChE. J.*, **46**, 416-426(2000).
10. Soorghali, F., Zolghadr, A. and Ayatollahi, S., "Effect of Native and Non-native Resins on Asphaltene Deposition and the Change of Surface Topography at Different Pressure: An Experimental Investigation," *Energy Fuels*, **29**(9), 5487-5494(2015).
11. León, O., Contreras, E., Rogel, E., Dambakli, G., Espidel, J. and Acevedo, S., "The Influence of the Adsorption of Amphiphiles and Resins in Controlling Asphaltene Flocculation," *Energy Fuels*, **15**(5), 1028-1032(2001).
12. LeÓn, O., Rogel, E., Urbina, A., Andújar, A. and Lucas, A., "Study of the Adsorption of Alkyl Benzene-derived Amphiphiles on Asphaltene Particles," *Langmuir*, **15**(22), 7653-7657(1999).
13. Junior, L. C. R., Ferreira, M. S. and da Silva Ramos, A.C., Inhibition of Asphaltene Precipitation in Brazilian Crude Oils Using New Oil Soluble Amphiphiles," *J. Pet. Sci. Eng.*, **51**(1-2), 26-36 (2006).
14. Chang, C.-L. and Fogler, H. S., "Stability of Asphaltene in Aliphatic Solvents Using Alkylbenzene-derived Amphiphiles. 1. Effect of the Chemical Structure of Amphiphiles on Asphaltene Stabilization," *Langmuir*, **10**(6), 1749-1757(1994).
15. Chang, C.-L. and Fogler, H. S., "Stability of Asphaltene in Aliphatic Solvents Using Alkylbenzene-derived Amphiphiles. 2. Study of the Asphaltene-amphiphile Interactions and the Structures Using Fourier Transform Infrared Spectroscopy and Small-angle X-ray Scattering Techniques," *Langmuir*, **10**(6), 1758-1766(1994).
16. Hashmi, S. M., Zhong, K. X. and Firoozabadi, A., "Acid-based Chemistry Enables Reversible Colloid-to-solution Transition of Asphaltenes in Non-polar Systems," *RSC Advances*, **8**, 8778-8785

(2012).
17. Goual, L. and Firoozabadi, A., "Effect of Resins and DBSA on Asphaltene Precipitation from Petroleum Fluids," *AIChE J.*, **50**, 470-479(2004).
18. Wei, D., Orlandi, E., Simon, S. and Sjöblom, J., "Interactions Between Asphaltenes and Alkylbenzene-derived Inhibitors Investigated by Isothermal Titration Calorimetry," *J. Therm. Anal. Calorim.*, **120**(3), 1835-1846(2015).
19. ASTM D 3279, Standard Test Method for n-Heptane Insolubles; ASTM International: USA, DOI: 10.1520/D3279-12E01.
20. Fan, T. and Buckley, J. S., "Rapid and Accurate SARA Analysis of Medium Gravity Crude Oils," *Energy Fuels*, **16**(6), 1571-1575(2002).
21. Fan, T., Wang, J. and Buckley, J. S., "Evaluating Crude Oils by SARA Analysis," *SPE/DOE Improved Oil Recovery Symposium*, April, Tulsa, DOI: 10.2118/75228-MS (2002).
22. Nelson, G. W., Perry, M., He, S.-M., Zechel, D. L. and Horton, J. H., "Characterization of Covalently Bonded Proteins on Poly (methyl methacrylate) by X-ray Photoelectron Spectroscopy," *Colloids Surf., B*, **78**(1), 61-68(2010).
23. Xu, X. F. and Zhang, P. Z., "The XPS Study of Forms of Oxygen, Nitrogen and Sulphur Elements in Gas Coal," *Coal Conversion (Meitan Zhuanhua)*, **19**(1), 72-77(1996).
24. Li, C., Wang, J. Q., Sui, L. T., Cui, M. and Deng, W. N., "Study on XPS of Venezuela Heavy Oil Asphaltene, *Acta Petrol Sin: Pet Process Section*, **29**(3), 459-463(2013).
25. Wang, J. Q., Li, C., Zhang, L. L., Que, G. H. and Li, Z. M., "The Properties of Asphaltenes and Their Interaction with Amphiphiles," *Energy Fuels*, **23**(7), 3625-3631(2009).
26. Abdallah, W. A. and Taylor, S. D., "Study of Asphaltene adsorption on Metallic Surface Using XPS and TOF-SIMS," *J. Phys. Chem. C.*, **112**(48), 18963-18972(2008).
27. Ramalho, J. B. V. S., Lechuga, F. C. and Lucas, E. F., "Effect of the Structure of Commercial Poly(ethylene oxide-b-propylene oxide) Demulsifier Bases on the Demulsification of Water-in-Crude Oil Emulsions: Elucidation of the Demulsification Mechanism, *Quim. Nova.*, **33**(8), 1664-1670(2010).
28. Mansur, C. R. E., de Melo, A. R. and Lucas, E. F., "Determination of Asphaltene Particle Size: Influence of Flocculant, Additive, and Temperature," *Energy Fuels*, **26**(8), 4988-4994(2012).
29. Pereira, J. C., López, I., Salas, R., Silva, F. and Fernández, C., "Resins: the Molecules Responsible for the Stability/instability Phenomena of Asphaltenes," *Energy Fuels*, **21**(3), 1317-1321(2007).
30. Pfeiffer, J. Ph. and Saal, R. N. J., "Asphaltene Bitumen as Colloid System," *J. Phys. Chem.*, **44**(2), 139-149(1940).
31. Alcázar-Vara, L. A., Zamudio, L. S. and Buenrostro-González, E., "Effect of Asphaltenes and Resins on Asphaltene Aggregation Inhibition, Rheological Behavior and Waterflood Oil-recovery," *J. Dispersion Sci. Technol.*, **37**(11), 1544-1554(2016).
32. Sun, Z.-H., Li, D., Ma, P.-P., Li, X.-K., Li, W.-H. and Zhu, Y.-H., "Characterization of Asphaltene Isolated from Low-temperature Coal Tar," *Fuel Process. Technol.*, **138**, 413-418(2015).
33. Seshadri, K. S., Young, D. C. and Cronauer, D. C., "Characterization of Coal Liquids by 13C N. M. R and FT-IR Spectroscopy-fractions Of Oils of SRC-I and Asphaltenes and Preasphaltenes of SRC-I and SRC-II," *Fuel*, **64**(1), 22-28(1985).
34. Mullins, O. C., Sheu, E. Y., Hammami, A. and Marshall, A. G., Asphaltenes, Heavy Oils, and Petroleomics, Springer, New York, 189-202(2007).
35. Andersen, S. I. and Christensen, S. D., "The Critical Micelle Concentration of Asphaltenes As Measured by Calorimetry," *Energy Fuels*, **14**(1), 38-42(2000).
36. Zhang, J., Qiu, Y. and Yu, D.-Y., "Critical Micelle Concentration Determination of Sodium Dodecyl Benzene Sulfonate by Synchronous Fluorescence Spectrometry," *Chin. J. Appl. Chem.*, **26**(12), 1480-1483(2009).
37. Somasundaran, P. and Zhang, L., "Adsorption of Surfactants on Minerals for Wettability Control in Improved Oil Recovery Processes," *J. Pet. Sci. Eng.*, **52**(1-4), 198-212(2006).